Supporting Information

Highly efficient CO_2 electrolysis to CO on Ruddlesden popper perovskite oxide with *in situ* exsolved Fe nanoparticles

*Junil Choi[a], Seongmin Park[a], Hyunsu Han[a], Minho Kim[a], Minseon Park[a], Jeonghyeon Han[a] and Won Bae Kim[a]**

[a] Department of Chemical Engineering, Pohang University of Science and Technology (POSTECH), 77 Cheongam-ro, Nam-gu, Pohang, Gyeongbuk, 37673, Republic of Korea

* Corresponding author
Tel: 82-54-279-2397
Fax: 82-54-279-5528
E-Mail: kimwb@postech.ac.kr

Table S1. Comparison of CO_2 electro-conversion performance to CO over ceramic-based cathodes with exsolved metal nanoparticles.

Catalyst	Exsolved element	Gas condition	Current density at 1.5 V ($A \cdot cm^{-2}$)	Faraday efficiency (%)	Reaction time (hour)	Ref
$\mathbf{La_{0.6}Sr_{0.4}Mn_{0.2}Fe_{0.8}O_3}$	Fe	30% CO/CO_2	2.04 (850 ℃)	97.9	100	**This work**
$\mathbf{Sr_{1.9}Fe_{1.5}Mo_{0.4}Ni_{0.1}O_{6-\delta}}$	Ni-Fe	100% CO_2	ca. 2.16 (800℃)	98	500	[S1]
$\mathbf{La_{0.6}Sr_{0.4}Fe_{0.8}Ni_{0.2}O_{3-\delta}}$	Ni-Fe	30% CO/CO_2	ca. 1.49 (850℃)	70	100	[S2]
$\mathbf{(La_{0.65}Sr_{0.3}Ce_{0.05})_{0.9}(Cr_{0.5}Fe_{0.5})_{0.85}Ni_{0.15}O_{3-\delta}}$	Ni-Fe	30% CO/CO_2	ca. 1.43 (850℃)	90.9	100	[S3]
$\mathbf{La_{0.6}Sr_{0.4}Co_{0.5}Ni_{0.2}Mn_{0.3}O_3}$	Co-Ni	30% CO/CO_2	1.08 (850℃)	97.8	90	[S4]
$\mathbf{La_{0.6}Sr_{0.4}Co_{0.7}Mn_{0.3}O_3}$	Co	30% CO/CO_2	1.03 (850℃)	97.4	12	[S5]
$\mathbf{Sr_2Fe_{1.35}Mo_{0.45}Ni_{0.2}O_{6-\delta}}$	$FeNi_3$	5% N_2/CO_2	ca. 0.890 (800℃)	97.5	40	[S6]
$\mathbf{Sr_2Fe_{1.58}Mo_{0.5}O_{6-\delta}}$	Fe	100 % CO_2	ca. 0.860 (850℃)	85	100	[S7]
$\mathbf{Pr_{0.4}Sr_{0.6}Co_{0.2}Fe_{0.7}Mo_{0.1}O_{3-\delta}}$	Co-Fe	100 % CO_2	ca. 0.830 (850℃)	87	100	[S8]
$\mathbf{(La_{0.2}Sr_{0.8})_{0.95}Ti_{0.85}Mn_{0.1}Ni_{0.05}O_{3+\delta}}$	Ni	100 % CO_2	ca. 0.440 (800℃)	96	100	[S9]
$\mathbf{(La_{0.75}Sr_{0.25})_{0.9}(Cr_{0.5}Mn_{0.5})_{0.9}Cu_{0.1}O_{3-\delta}}$	Cu	100 % CO_2	ca. 0.235 (800℃)	65	-	[S10]
$\mathbf{(La_{0.75}Sr_{0.25})_{0.9}(Cr_{0.5}Mn_{0.5})_{0.9}Ni_{0.1}O_{3-\delta}}$	Ni	100 % CO_2	ca. 0.190 (800℃)	80	21	[S11]

Temperature (℃)	R_1 ($\Omega \cdot cm^2$)	R_2 ($\Omega \cdot cm^2$)
850	0.033	0.169
800	0.120	0.218
750	0.288	0.324

Table S2. Values of polarization resistance component in fitted equivalent circuit at OCV.

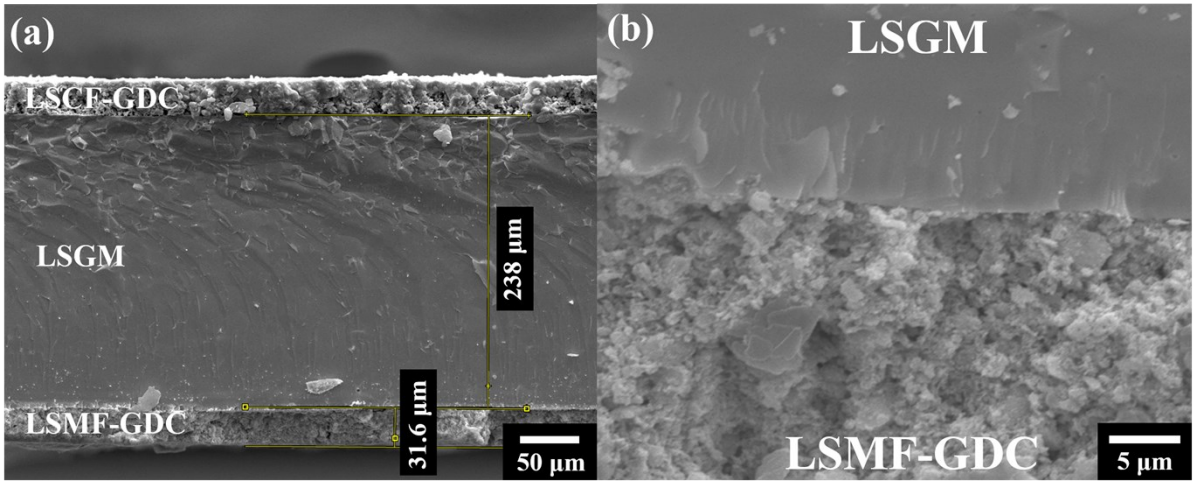

Fig S1. The SEM image of (a) cross-section of button cell (LSMF-GDC|LSGM|LSCF-GDC) and (b) porous structure of LSMF-GDC electrode.

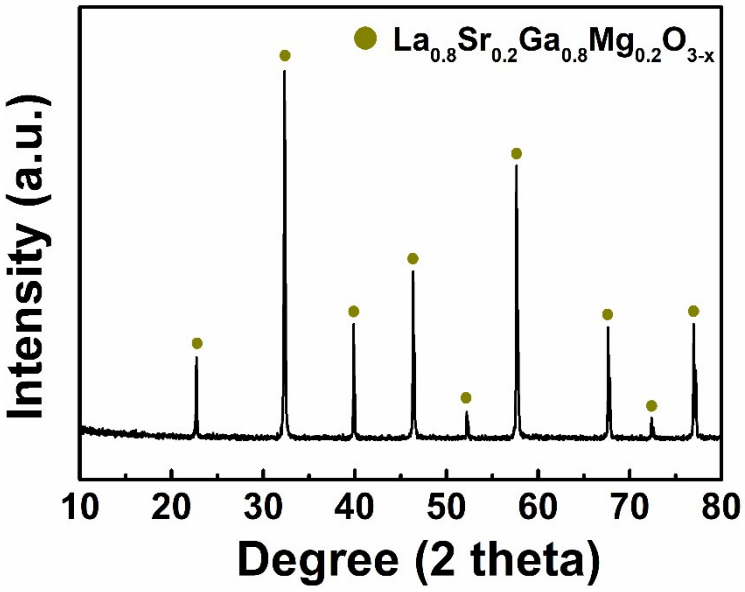

Fig S2. XRD pattern of grounded LSGM pellet measured after twice-sintered process (XRD measurement condition: 40kV and 30 mA).

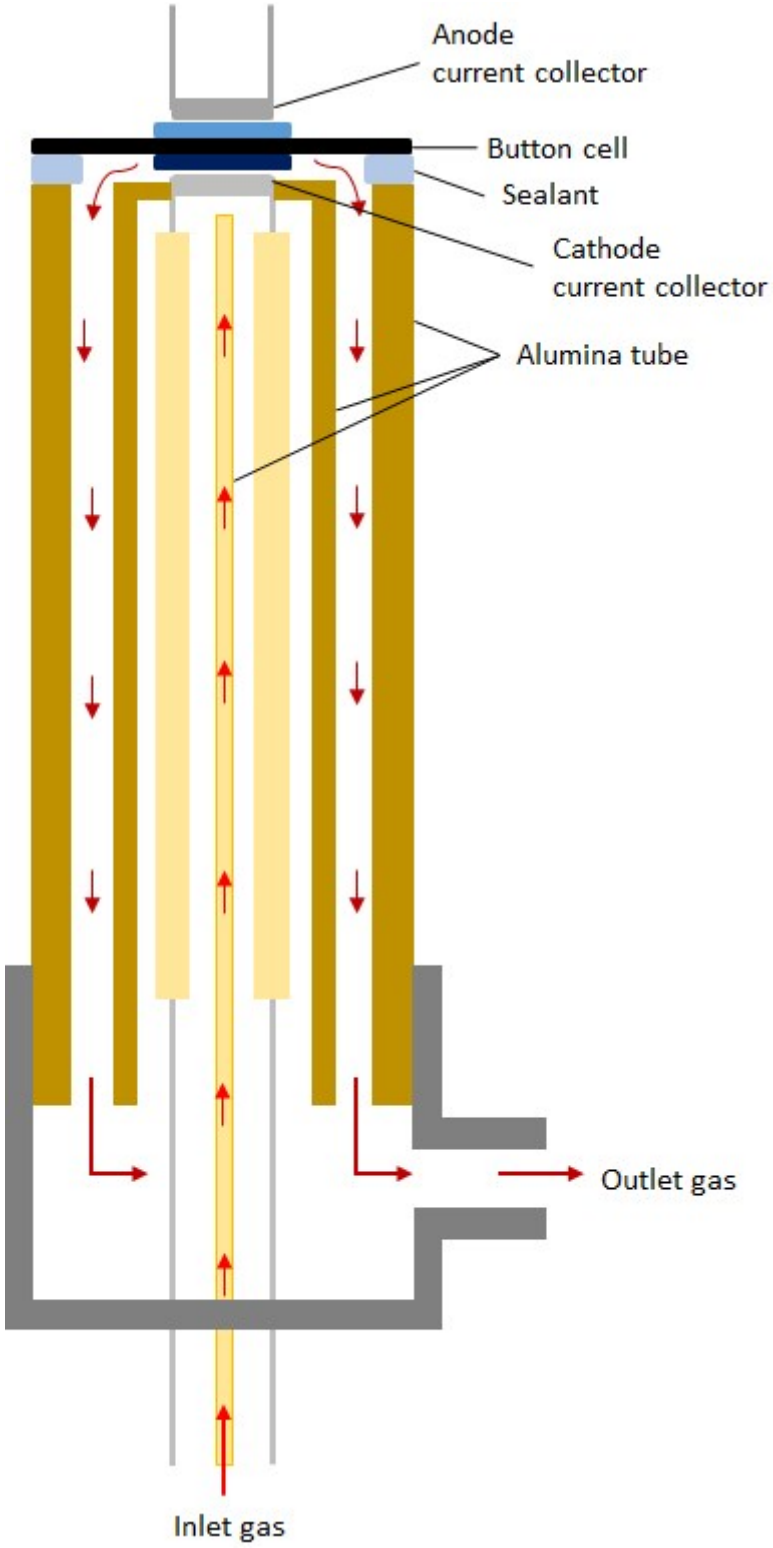

Fig S3. Schematic diagram of SOEC test reactor for high temperature CO_2 electrolysis.

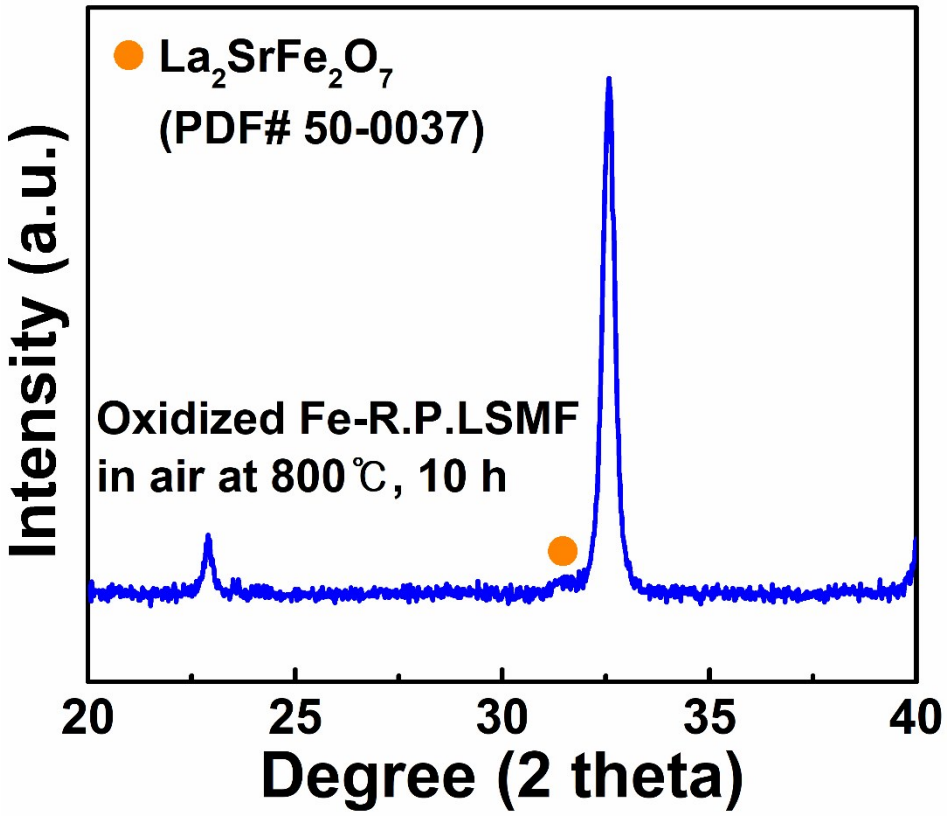

Figure S4. XRD pattern of oxidized Fe-R.P.LSMF in the 2θ range from 20 º to 40 º.

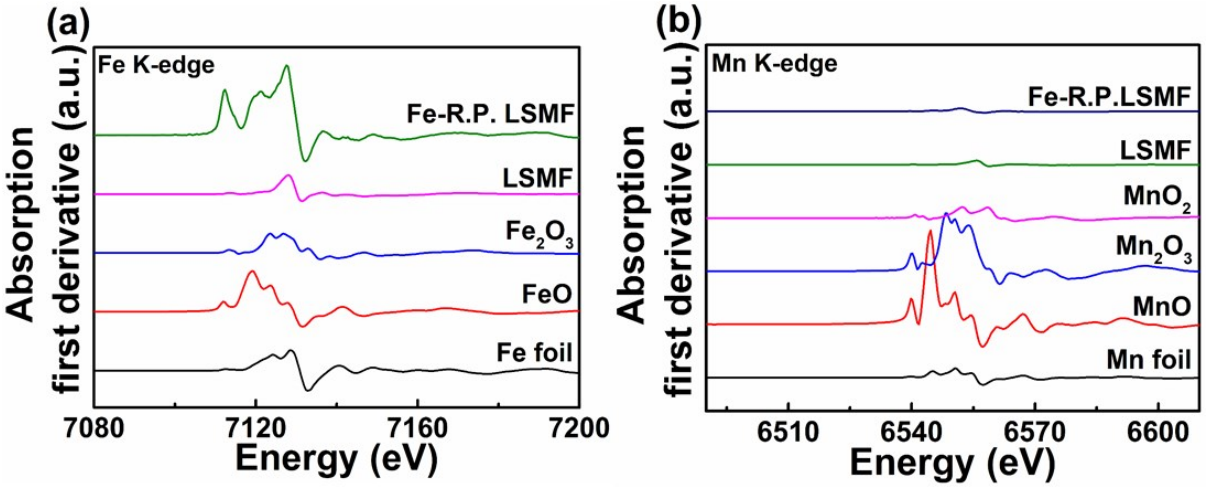

Fig S5. First derivatives of (a) Fe K-edge and (b) Mn K-edge XANES spectra of reference oxides, LSMF and Fe-R.P.LSMF.

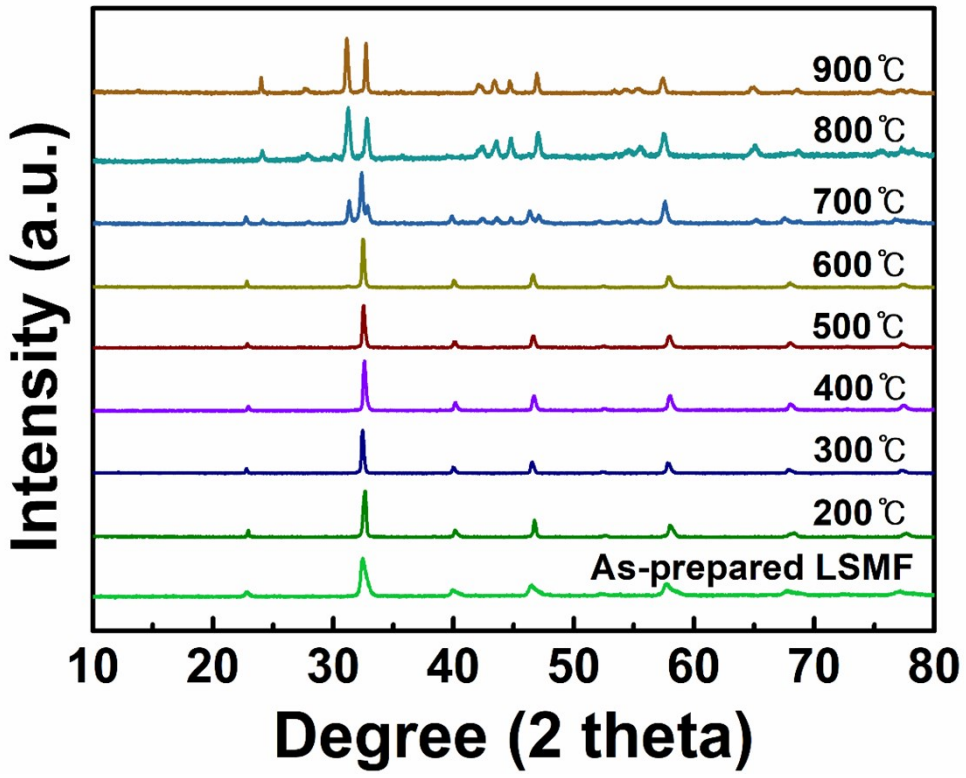

Fig S6. XRD patterns of LSMF after treated in 20% H_2/N_2 atmosphere from room temperature to 900 ℃.

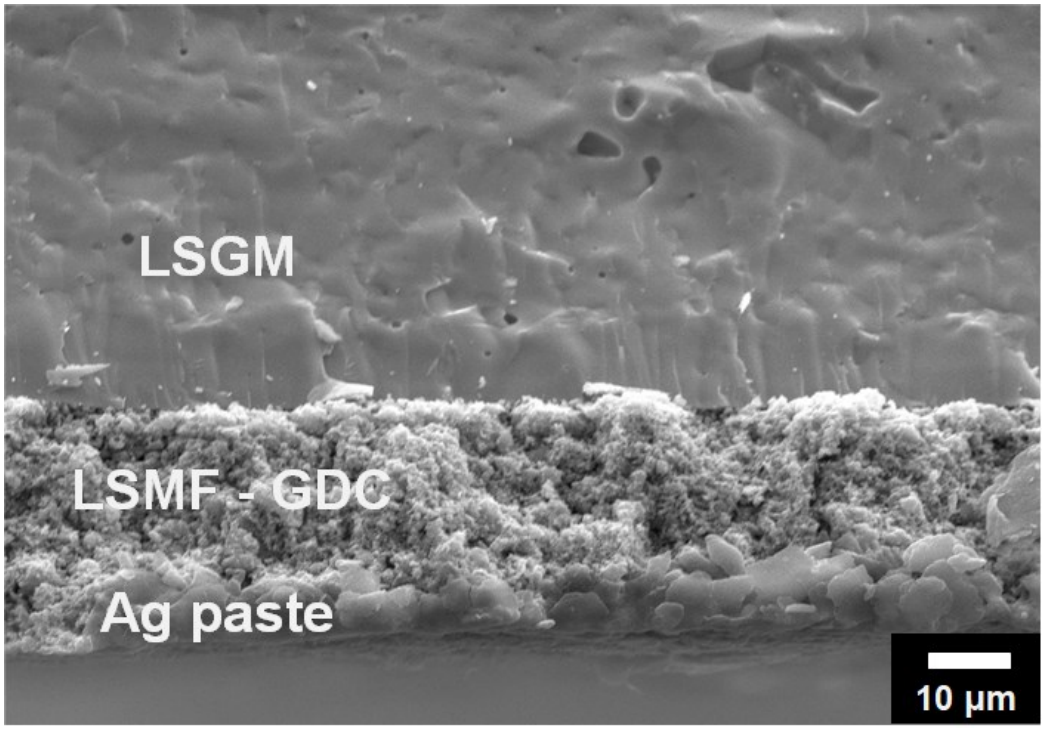

Figure S7. The cross-sectional SEM image of button cell after reduction process.

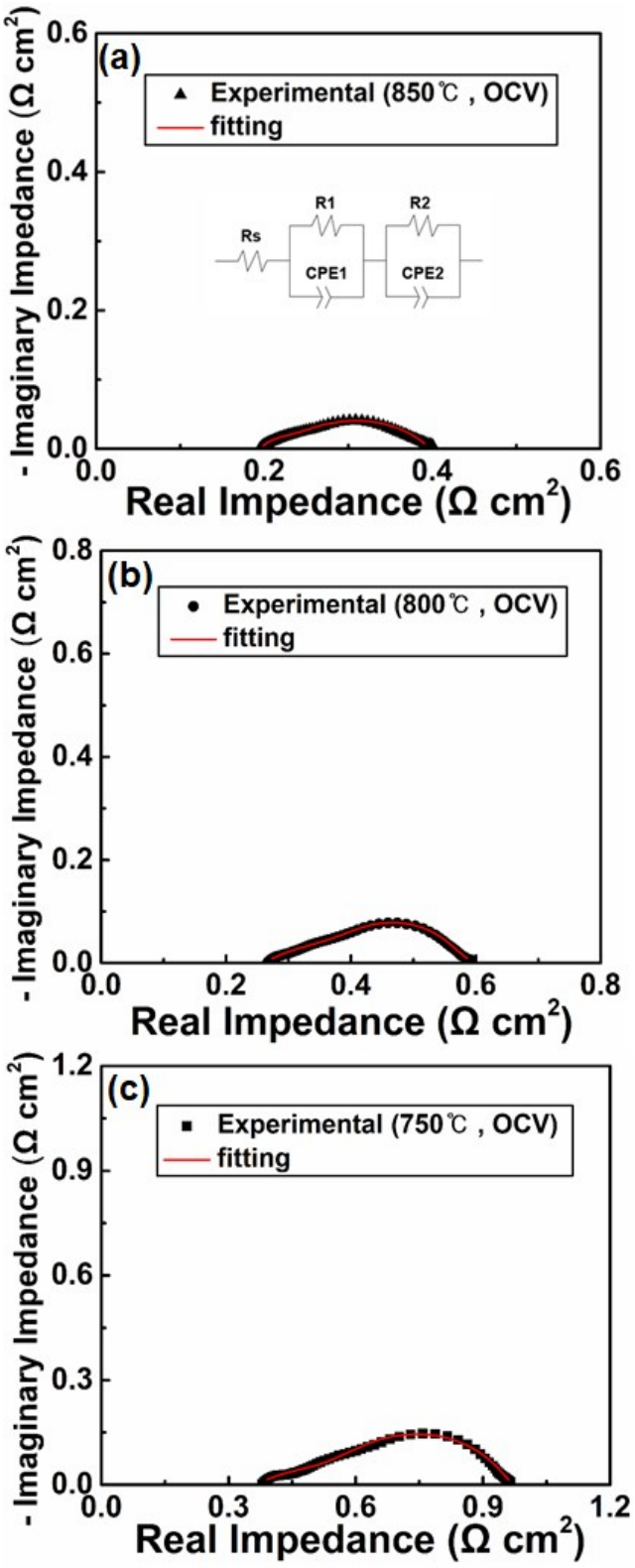

Fig S8. EIS profiles and its fitted data of inserted equivalent circuit at OCV with respect to temperatures of (a) 850 ℃, (b) 800 ℃, and (c) 750 ℃.

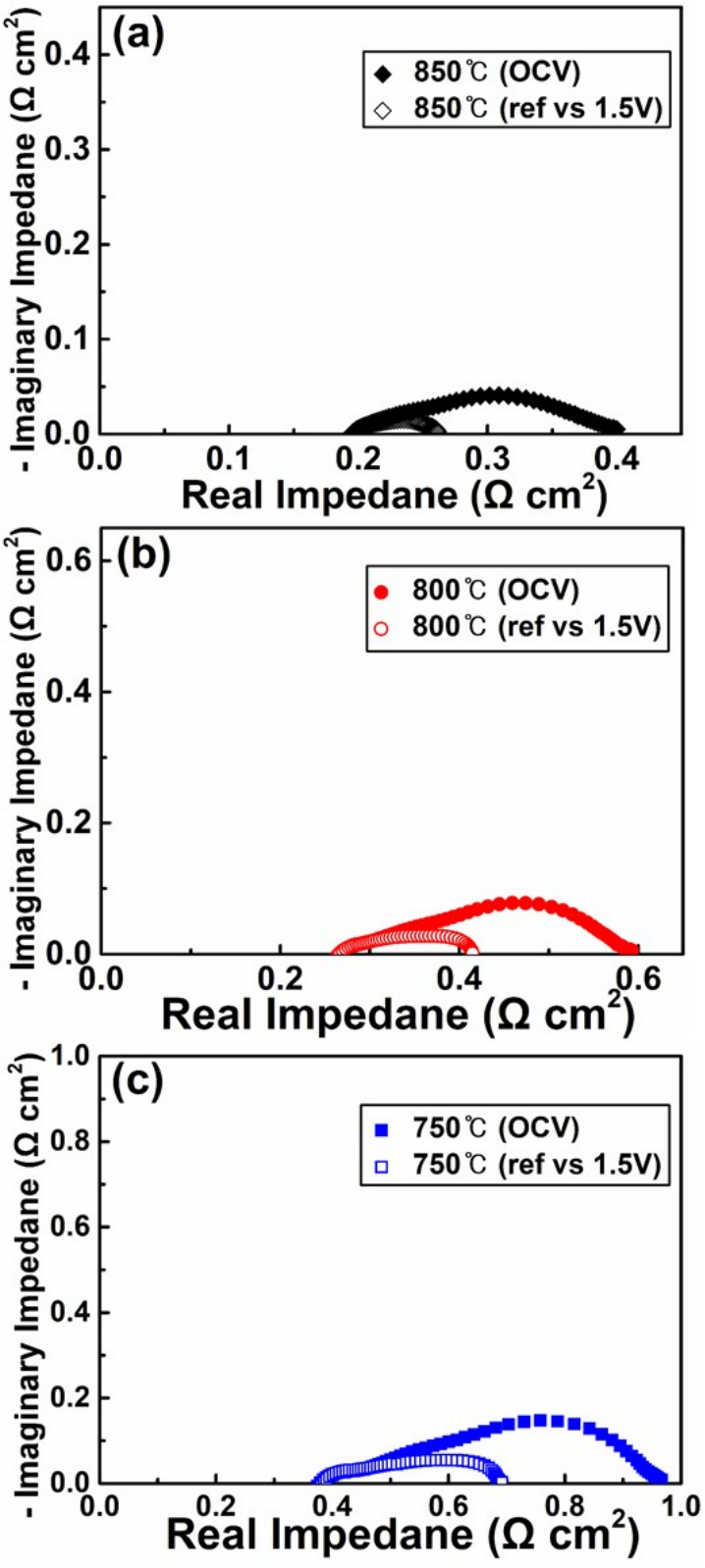

Fig S9. EIS profiles under OCV and operating voltage of 1.5 V at temperatures of (a) 850 ℃, (b) 800 ℃, and (c) 750 ℃.

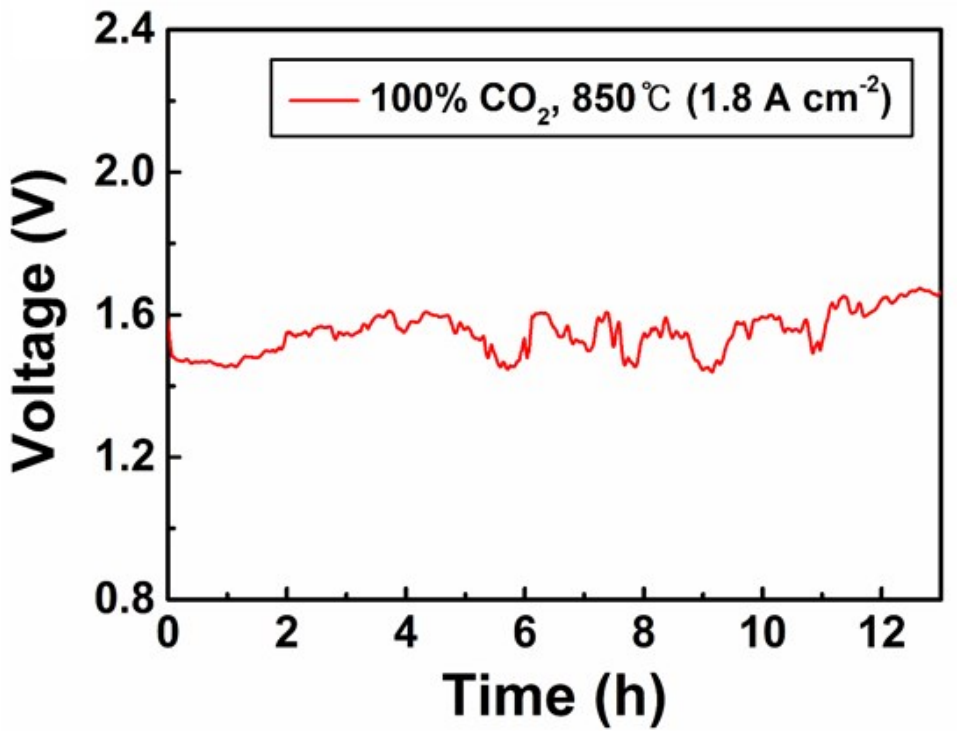

Fig S10. The voltage profile of the button cell during 13h operation with an applied constant current of 1.8 A·cm^{-2} in a pure CO_2 at 850 ℃.

Reference

[S1]Y. Li, B. Hu, C. Xia, W. Q. Xu, J. P. Lemmon, F. Chen, *J. Mater. Chem. A*, 2017, 5, 20833-20842.

[S2]S. Liu, Q. Liu, J. L. Luo, *ACS Catal.,* 2016, 6, 6219-6228.

[S3]S. Ding, M. Li, W. Pang, B. Hua, N. Duan, Y. Q. Zhang, S. N. Zhang, J. L. Luo, *Electrochim. Acta*, 2020, 335, 135683.

[S4]S. Park, Y. Kim, Y. Noh, T. Kim, H. Han, W. Yoon, J. Choi, S. Yi, W. Lee, W. B. Kim, *J. Mater. Chem. A*, 8, 138-148.

[S5]S. Park, Y. Kim, H. Han, Y. S. Chung, W. Yoon, J. Choi, W. B. Kim, *Appl. Catal. B-Environ.*, 2019, 248, 147-156.

[S6]H. Lv, L. Lin, X. Zhang, D. Gao, Y. Song, Y. Zhou, Q. Liu, G. Wang, X. Bao, *J. Mater. Chem. A*, 2019, 7, 11967-11975.

[S7]L. Chen, J. Xu, X. Wang, K. Xie, *Int. J. Hydrog. Energy*, 2020, 45, 11901-11907

[S8]S. Liu, Q. Liu, J. L. Luo, *J. Mater. Chem. A*, 2016, 4, 17521-17528.

[S9]L. Ye, M. Zhang, P. Huang, G. Guo, M. Hong, C. Li, J. T. Irvine, K. Xie, *Nat. Commun.*, 2017, 8, 14785.

[S10]H. Li, G. Sun, K. Xie, W. Qi, Q. Qin, H. Wei, S. Chen, Y. Wang, Y. Zhang, Y. Wu, *Int. J. Hydrog. Energy*, 2014, 39, 20888-20897.

[S11]C. Ruan, K. Xie, *Catal. Sci. Technol.*, 2015, 5, 1929-1940.